

## Supporting Information

for *Adv. Sci.*, DOI 10.1002/adv.202106115

Polyglutamic Acid-Based Elastic and Tough Adhesive Patch Promotes Tissue Regeneration through In Situ Macrophage Modulation

*Qiuwen Zhu, Yi Hong, Yuxuan Huang, Yi Zhang, Chang Xie, Renjie Liang, Chenglin Li, Tao Zhang, Hongwei Wu, Jinchun Ye, Xianzhu Zhang, Shufang Zhang, Xiaohui Zou\* and Hongwei Ouyang\**

Supplementary Materials for

**Polyglutamic acid-based elastic and tough adhesive patch promotes tissue  
regeneration through in situ macrophage-modulation**

*Qiuwen Zhu<sup>1,2,3,‡</sup>, Yi Hong<sup>1,2,3,‡</sup>, Yuxuan Huang<sup>1,2,3</sup>, Yi Zhang<sup>1,2,3</sup>, Chang Xie<sup>1,2,3</sup>, Renjie Liang<sup>1,2,3</sup>,  
Chenglin Li<sup>1,2,3</sup>, Tao Zhang<sup>1,2,3</sup>, Hongwei Wu<sup>1,2,3</sup>, Jinchun Ye<sup>1,2,3</sup>, Xianzhu Zhang<sup>1,2,3</sup>, Shufang  
Zhang<sup>1,2,3,5</sup>, Xiaohui Zou<sup>1,3,4,\*</sup>, Hongwei Ouyang<sup>1,2,3,5,\*</sup>*

‡These authors contributed equally to this work.

**Figure S1.**  
**The final package of the LAP.**



**Figure S2.**

**The top view (a) and side view (b) of the matrix hydrogel, NB-modified matrix hydrogel and the dried LAP with different concentration of the PGA.**

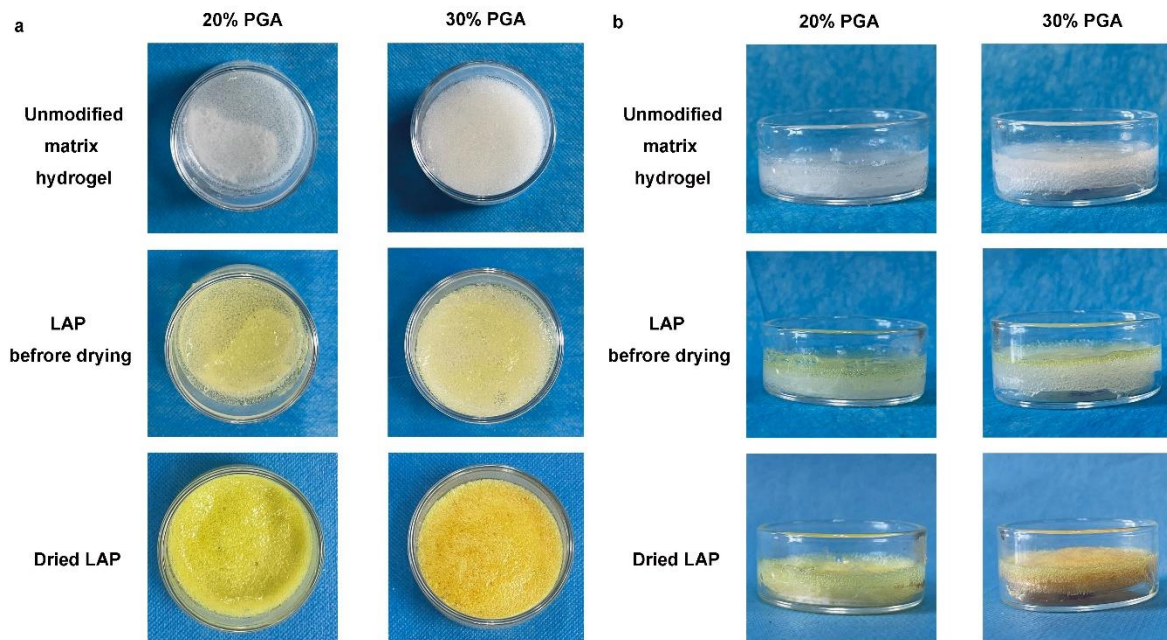


**Figure S3.**

**Water absorption ratio of matrix hydrogel synthesized by different concentration of the PGA.** Values represent the mean and the standard deviation (n=3). P value were determined by t-student test; \*\*\* $p < 0.001$ .

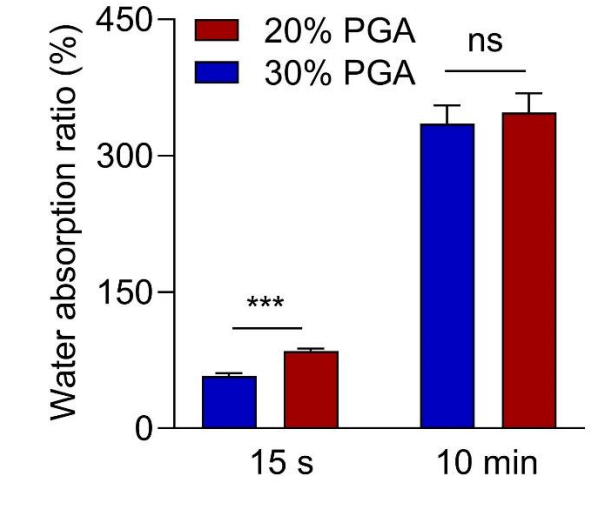


**Figure S4.**

**Pull-off strength of LAP at different feeding ratio of the carboxyl group in PGA to the amino group in PLA (PGA: PLA).** Values represent the mean and the standard deviation (n=3). P value were determined by one way ANOVA; \*\*\*\* $p < 0.0001$ .

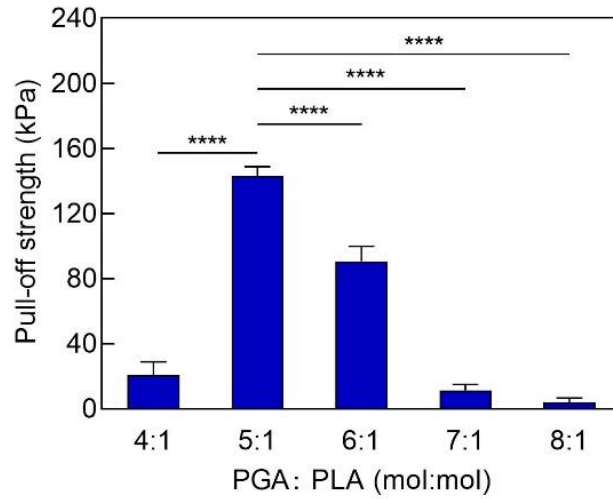


**Figure S5.**

**Survey XPS spectra of PLA treated PLLA base film with (PLLA+PLA+END/NHS) or without (PLLA+PLA) coupling reagents, and untreated PLLA base film (PLLA).** The survey XPS spectra of the PLLA+PLA+END/NHS clearly exhibit N1s peaks at a binding energy of 399.23eV, whereas the PLLA+PLA show a negligible N1s peaks and the PLLA does not have any N1s peaks in the corresponding energy range.

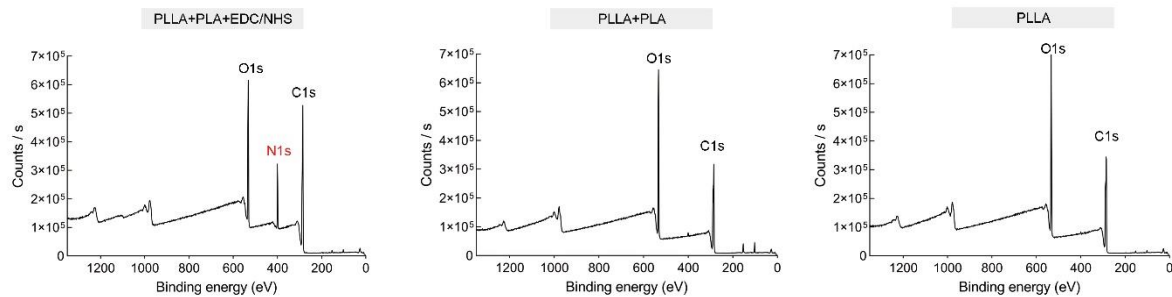


**Figure S6.**  
**The stress-strain curve of the matrix hydrogel and LAP.**

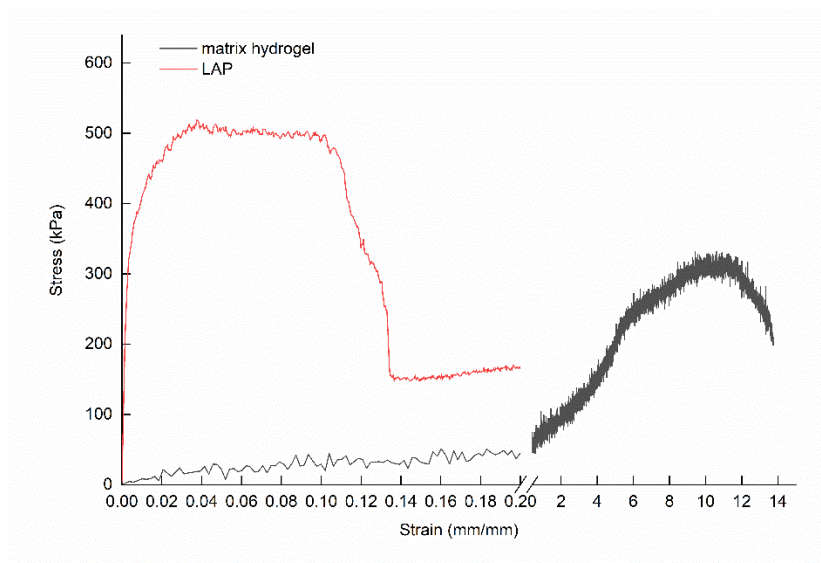




**Figure S7.**

**FTIR spectra of the surface of the LAP before and after UV irradiation.**

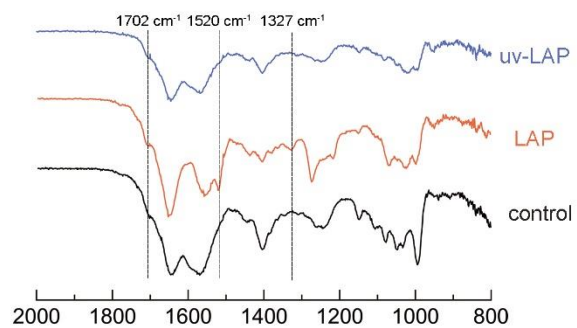


**Figure S8.**

**Representative force curves of the LAP adhere to wet porcine muscle. a,** pull-off strength vs. displacement curves for tensile tests of porcine muscle adhered by the LAP and cyanoacrylate. **b,** Force/width vs. displacement curves for 180-degree peeling tests of wet porcine muscle adhered by the LAP. **c,** Shear stress vs. displacement curves for lap-shear tests of wet porcine muscle adhered by the LAP.

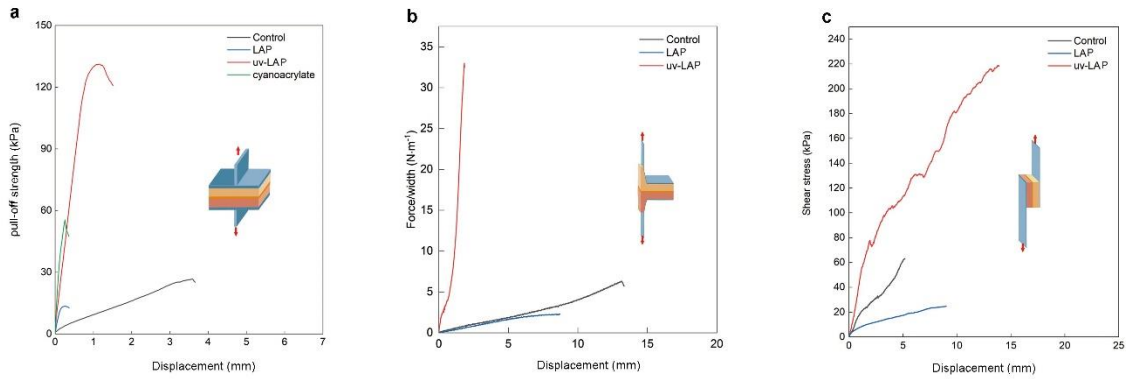


**Figure S9.**

**Robust adhesion of the LAP on the surface of wet porcine muscle. a,** The stretched LAP during the coating adhesion test and the broken LAP after the test. The broken LAP attached to the tissue surface. **b,** Coating adhesion test on NB-modified matrix hydrogel without base film. The fracture turned to be the internal connection of the matrix hydrogel.

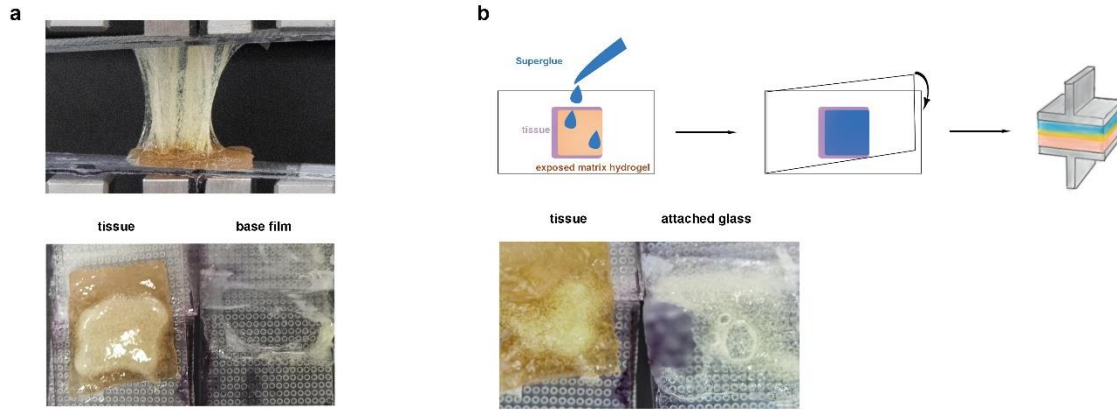


**Figure S10.**

**Biodegradation testing of LAP after subcutaneous implantation.** **a**, Schematic illustration of subcutaneous implantation with LAP. **b**, Degradation curve of LAP after implantation over time. (n=6)

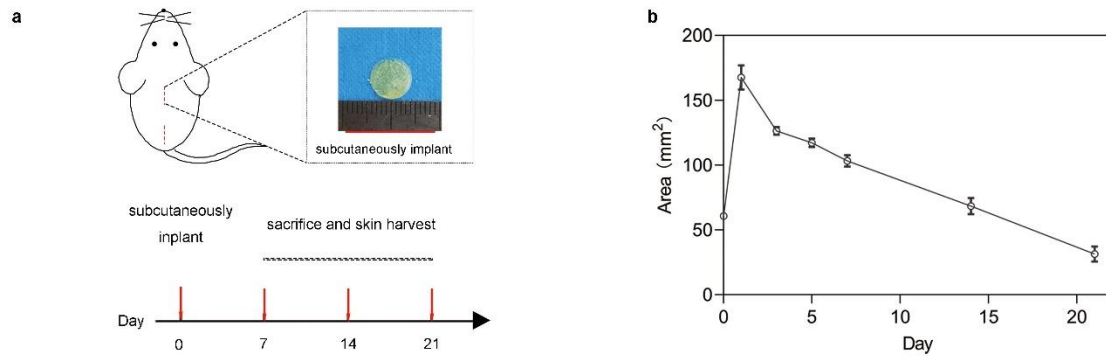


**Figure S11.**

**Macroscopic view of LAP and cyanoacrylate implants** at 1, 2 and 4 weeks post-implantation.  
(the red dotted circles point out the remaining implants)

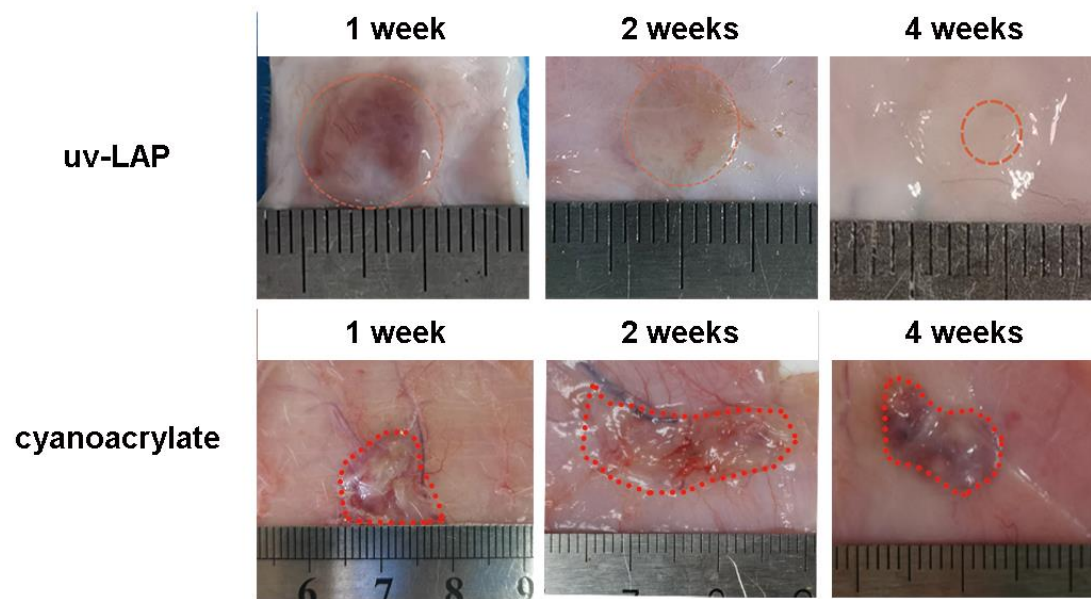


**Figure S12.**

Confocal imaging of immunofluorescence-stained LAP 1,2, and 4 weeks post subcutaneous implantation. Cell nuclei are stained with DAPI (blue). Red fluorescence corresponds to the expression of CD31<sup>+</sup> cells. White dashed line indicates the boundary of the implanted sample (scale bar 50 $\mu$ m).

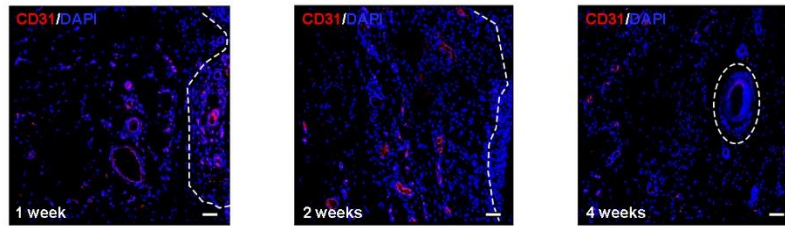


**Figure S13.**

**In vivo application based on gastric perforation model.** **a**, 8 mm diameter Gastric perforation model in rabbit was created by scissors. **b**, Survival of rabbits after gastric perforation rabbits treated with LAP, suture and cyanoacrylate. **c**, Anatomy of stomach from dead rabbits treated by suture and cyanoacrylate.

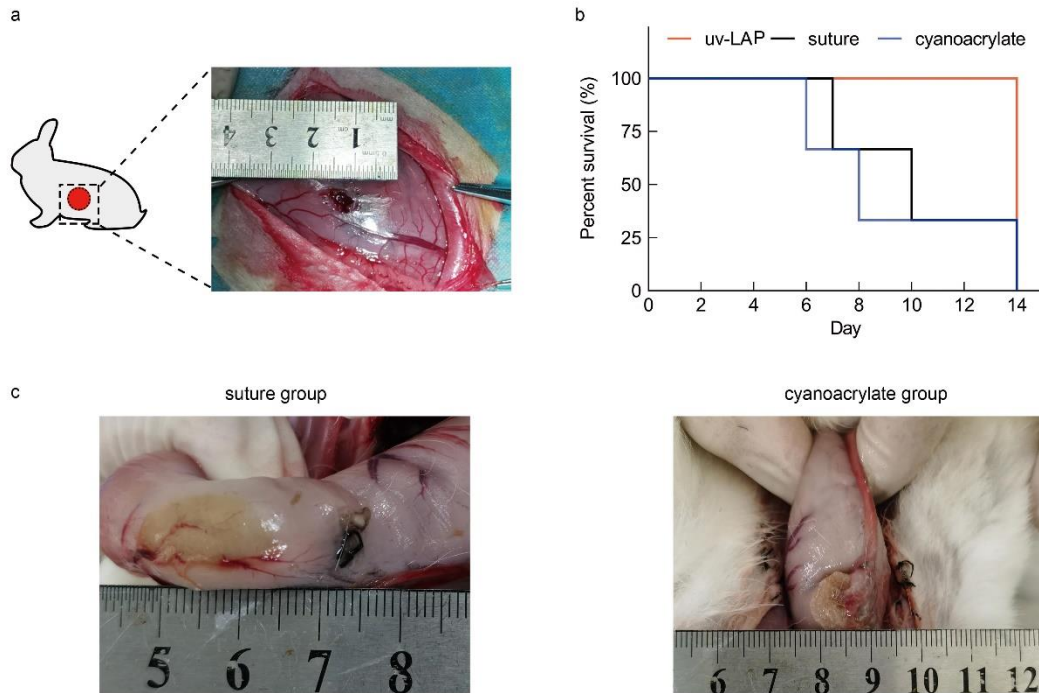


**Figure S14.**

**Microscopic images of H&E staining.** The images show the histological analysis of whole layer repair (up, scale bar 400  $\mu\text{m}$ ) and the regeneration of the muscularis and mucosa in the middle area of the gastric perforation (down, scale bar 100  $\mu\text{m}$ ) after treated by b) uv-LAP, c) suture, and d) cyanoacrylate. Unpunctured stomach is served as a positive control and dotted line represents the damaged area.

